Melamine-supported nickel oxide nanoparticles as a good alternative to conventional copper catalysts for the regioselective synthesis of triazole derivatives in water

Zahra Hashemi[1] · Jalal Albadi[1] · Mehdi Jalali[2]

Abstract

Nickel oxide nanoparticles supported on melamine as a good alternative to conventional copper catalysts have been prepared and used for the regioselective synthesis of triazole derivatives in water. This catalyst can be reused several times without any significant decrease in the catalytic activity. The nanocatalyst was characterized by Fourier transform infrared spectroscopy (FT-IR), thermogravimetric analysis (TGA), field emission scanning electron microscopy (FESEM), energy-dispersive spectroscopy (EDS), X-ray diffraction (XRD), transmission electron microscopy (TEM), inductively coupled plasma (ICP), X-ray fluorescence (XRF) and Brunauer–Emmett–Teller (BET) surface area analysis.

Introduction

The copper-catalyzed synthesis of triazole derivatives has gained a great amount of attention because of diversity in pharmacological activities, medicinal chemistry, materials science, and chemical biology [1]. The main procedure for the synthesis of triazoles is the Huisgen 1,3-dipolar cycloaddition reaction of azides with alkynes, which has developed the typical for click reactions [2].

✉ Jalal Albadi
chemalbadi@gmail.com; albadi@sku.ac.ir

1 Department of Chemistry, College of Science, Shahrekord University, Shahrekord, Iran

2 Petrochemical Research and Technology Company, National Petrochemical Company, Tehran, Iran

In general, catalysts based on Cu (I) or Cu (II) are used for the synthesis of triazole derivatives [3–14]. Also, some catalysts derived from Ag, Au, Al, Ru, and Ir are used to promote the synthesis of these compounds [15–19]. Moreover, in the previous research, the use of limited number nickel catalysts has been reported for the synthesis of triazole derivatives. Rao and co-workers reported the Raney nickel-catalyzed synthesis of triazole derivatives [20]. However, one of the main disadvantages in this method is to perform reactions in toluene as a dangerous organic solvent. Moreover, Kim et al. reported the Cp_2Ni-catalyzed azide-alkyne cycloaddition (NiAAC), obtaining a variety of 1,5-disubstituted 1,2,3-triazoles [21]. Although synthesis of triazole derivatives in the presence of Cp_2Ni is well done, the reactions performed in the presence of the Cs_2CO_3 and xantphos as additive reagents under air. Furthermore, the catalysts are difficult to make. Therefore, preparation of a new, simple, and efficient nickel-based catalyst may afford a prospect to extend the new catalytic system with useful high-performance applications.

Use of supported-metallic nanoparticles as catalysts has attracted significant experimental attention on the organic synthesis [22–26]. It is demonstrated that the immobilization of metallic nanoparticles on the high-surface-area supports allows a higher stability and dispersion of the particles, selectivity, easier work-up and recycling properties of the catalyst [27].

Melamine (2,4,6-triamino-1,3,5-triazine), due to having nitrogen in its structure and high loading capacity, can be used as a simple and efficient support for the nickel catalysts. Therefore, in continuation of our researches on the development of novel nanocatalysts [28–32], we decided to use the melamine as a support for the preparation of melamine-supported nickel oxide nanoparticles (M-NiO nanocatalyst) as a new, simple and efficient catalyst for the regioselective synthesis of 1,4-disubstituted-1,2,3-triazoles in water (Scheme 1). M-NiO nanocatalyst as a recyclable nanocatalyst is safe, stable, easy to handle, environmentally benign, and its preparation is straightforward.
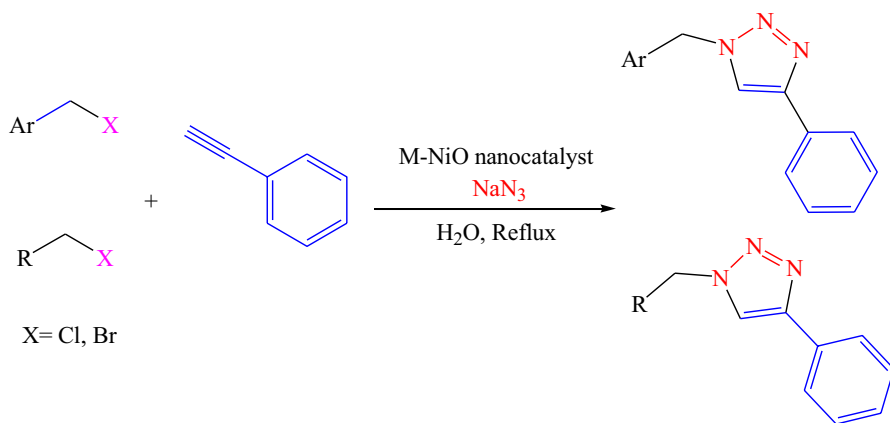
Scheme 1 Regioselective synthesis of triazole derivatives catalyzed by M-NiO nanocatalyst in water

Experimental

Chemical materials were purchased from Merck chemical companies. Prepared products were characterized by the evaluation of their spectroscopic data such as nuclear magnetic resonance and Fourier transform infrared spectroscopy (NMR, FT-IR) as well as physical properties with those reported in the literature. The morphology and size of the nanocatalyst were studied by field emission scanning electron microscopy (FESEM) method by a TESCAN MIRA3 instrument, equipped with an energy-dispersive spectroscopy (EDS) analytical system. Transmission electron microscopy (TEM) analysis was also performed using a Philips EM 208S (100 kV) microscope. Thermal decomposition behavior of prepared nanocatalyst was determined using thermogravimetric analysis (TGA) by TA-Q600 instrument. The XRD investigation was performed using an X-ray diffractometer, Cu-Kα monochromatized radiation source and a nickel filter (Panalytical X'Pert-Pro). The average crystallite size of the sample was calculated using the Scherrer equation. The BET surface area was tested by N_2 adsorption–desorption method. The analysis was carried out using an automated gas adsorption analyzer (Tristar 3020, Micromeritics). The sample was purged with nitrogen gas for 3 h at 300 °C by a VacPrep 061 degas system (Micromeritics).

Catalyst preparation

The M-NiO nanocatalyst was prepared by a co-precipitation method. Aqueous solution of Na_2CO_3 (0.5 M) was added dropwise into a mixture of melamine (3 g) and 0.015 M $Ni(NO_3)_2.6H_2O$, under vigorous stirring, while temperature was fixed at 60 °C. The obtained sample was filtered and washed with deionized water. It was dried for 12 h at 100 °C, followed by calcination at 3000 °C for 3 h to obtain the final nanocatalyst.

General procedure

Alkyne (1.1 mmol), benzyl halide or alkyl halide (1 mmol), sodium azide (1.1 mmol), and M-NiO nanocatalyst (0.03 g) were added to round-bottom flask containing 10 mL of water. The mixture was stirred under reflux condition. The progress of the reactions was monitored by TLC (*n*-hexane: ethyl acetate; 4:1). After reaction completion, the reaction mixture was cooled and the catalyst filtered. Then, the recovered catalyst was washed with hot ethanol, dried and stored for another following reaction run. The filtrate was evaporated to dryness, and the obtained solid was recrystallized in ethanol/water (3:1 v/v) to afford the desired pure products in high yields.

Results and discussion

Catalyst characterization

The nanocatalyst was characterized by Fourier transform infrared spectroscopy (FT-IR), thermogravimetric analysis (TGA), field emission scanning electron microscopy

(FESEM), energy-dispersive spectroscopy (EDS), X-ray diffraction (XRD), transmission electron microscopy (TEM), inductively coupled plasma (ICP), X-ray fluorescence (XRF) and Brunauer–Emmett–Teller (BET) surface area analysis. The XRD patterns of the M-NiO nanocatalyst and the melamine support are shown in Fig. 1. The melamine shows diffraction peaks at $2\theta = 12.9$, $2\theta = 14.7$, $2\theta = 17.7$, $2\theta = 21.5$, $2\theta = 22.08$, $2\theta = 26.07$, $2\theta = 27.05$, $2\theta = 28.8$ and $2\theta = 29.8$ which are attributed to [100], [011], [110], [112], [012], [021], [200], [212], and [210] crystalline planes of melamine [33, 34]. The diffraction peaks at $2\theta = 38.2$, $2\theta = 43.8$, $2\theta = 62.6$, $2\theta = 76.14$ and $2\theta = 79.41$, respectively, correspond to [111], [200], [220], [311] and [222] crystalline planes of NiO [35]. The mean particle size was calculated based on the Debbie-Scherer relationship according to the peak with the highest intensity for melamine, and catalyst was 27.16 and 20.97 nm, respectively.

Figure 2 displays FESEM micrographs, EDS results for the M-NiO nanocatalyst and melamine support. FESEM analysis (Fig. 2b) shows the presence of spherical NiO nanoparticles with a diameter of less than 40 nm on the outside surface of melamine support. Comparison of elemental analysis of melamine and M-NiO catalyst nanoparticles (Fig. 2 c, d) shows the presence of elements related to each without the presence of other additional elements. At the same time, the amount of nickel in the sample was 7.87 w w^{-1}. It is in agreement with the results obtained by ICP (7.96% w w^{-1}) and X-ray fluorescence (7.99% w w^{-1}).
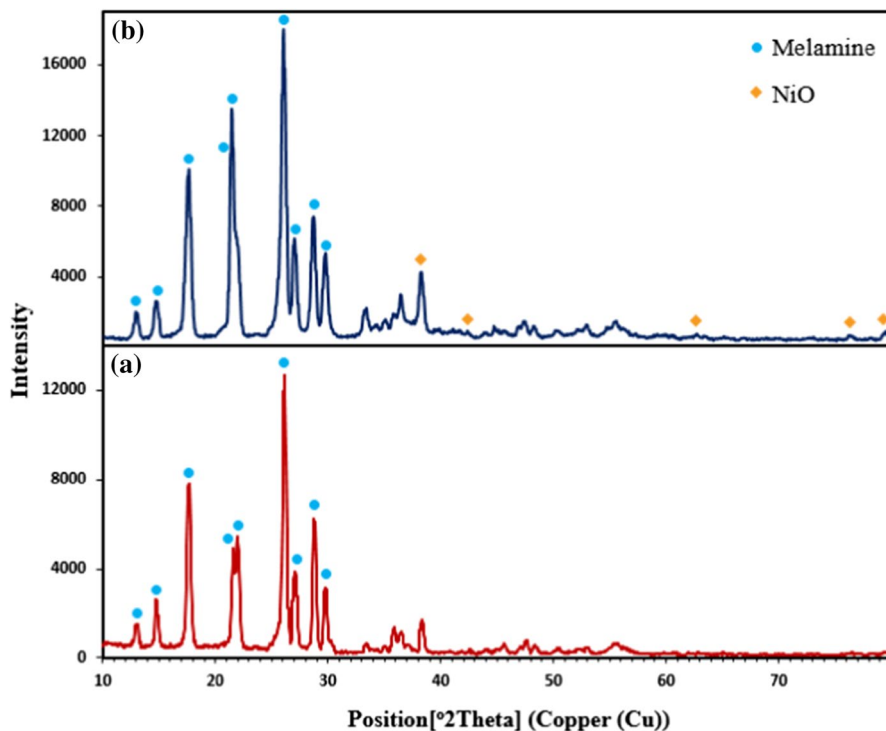

Fig. 1 The XRD pattern of melamine (**a**) and M-NiO nanocatalyst (**b**)

Figure 3 (a) shows the nitrogen adsorption–desorption isotherm of the melamine support and M-NiO nanocatalyst. The results display that both the support and the catalyst show an adsorption/desorption isotherm profile with a hysteresis loop H3 between $P/P_0 = 0.3$ and 0.98. According to the IUPAC classification, this type of isotherms is ascribed to mesoporous structures and can be categorized as type IV.

Table 1 shows the information of support and the nanocatalyst. As can be seen in the table, the BET surface area and total pore volume of nanocatalyst with respect to the melamine support increased and the pore diameter of it decreased and this indicates the presence of NiO nanoparticles on the melamine. Figure 3 (b) exhibits a narrow pore size distribution for both the melamine and the M-NiO catalyst with a maximum at about 7 and 6 nm, respectively.

Transmission electron microscopy (TEM) images are shown in Fig. 4. Results of the TEM images show uniform distribution of the NiO nanoparticles on the melamine surface.

In order to reveal the changes that occurred during heat treatment of the precursor powders, TGA–DSC study was carried out from 25 to 500 °C in the atmosphere. Figure 5 (a) shows the TGA curve of M-NiO including one step of weight loss in a temperature range of 300–360 °C that can be attributed to the decomposition of precursor materials. This finding suggests that the precursor decomposed completely at 360 °C to become nickel oxide. Meanwhile, endothermic (53 °C and 358 °C) peaks were observed in differential scanning calorimetry (DSC) and
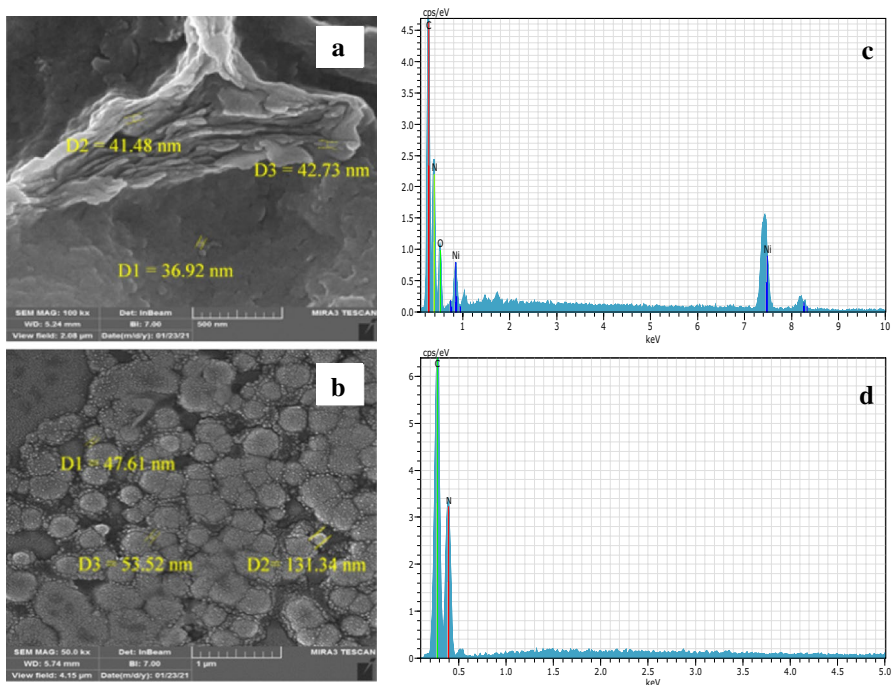

Fig. 2 FESEM micrographs of M-NiO (**a**) and melamine (**b**), EDX results of M-NiO (**c**) and melamine (**d**)
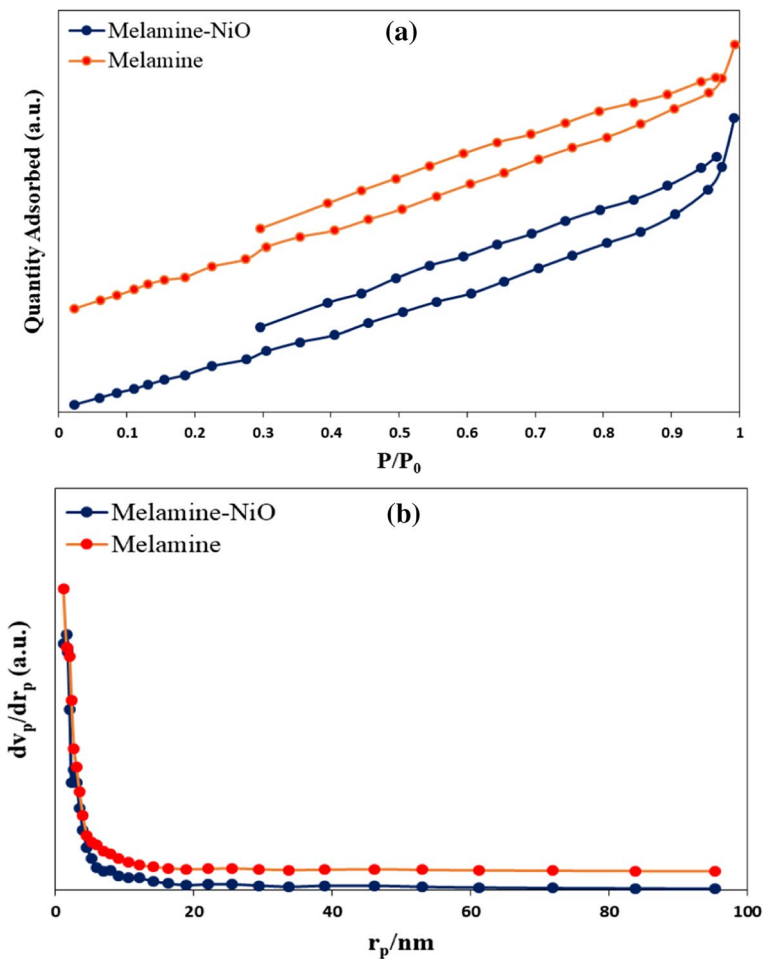
Fig. 3 N_2 adsorption/desorption isotherm (**a**) and average pore size distributions (**b**) of melamine and M-NiO nanocatalyst

Table 1 Structural properties of the melamine and M-NiO nanocatalyst

Sample	BET surface area ($m^2\,g^{-1}$)	Average pore diameters (nm)	Pore volume ($cm^3\,g^{-1}$)
Melamine	4.36	7.38	0.008
M-NiO nanocatalyst	5.71	6.19	0.0088

differential thermal analysis (DTA) curves (Fig. 5 a, b). The endothermic reaction in 53 °C was attributed to the decomposition of water, whereas the endothermic reaction in 358 °C happened because of decomposition of precursor materials.
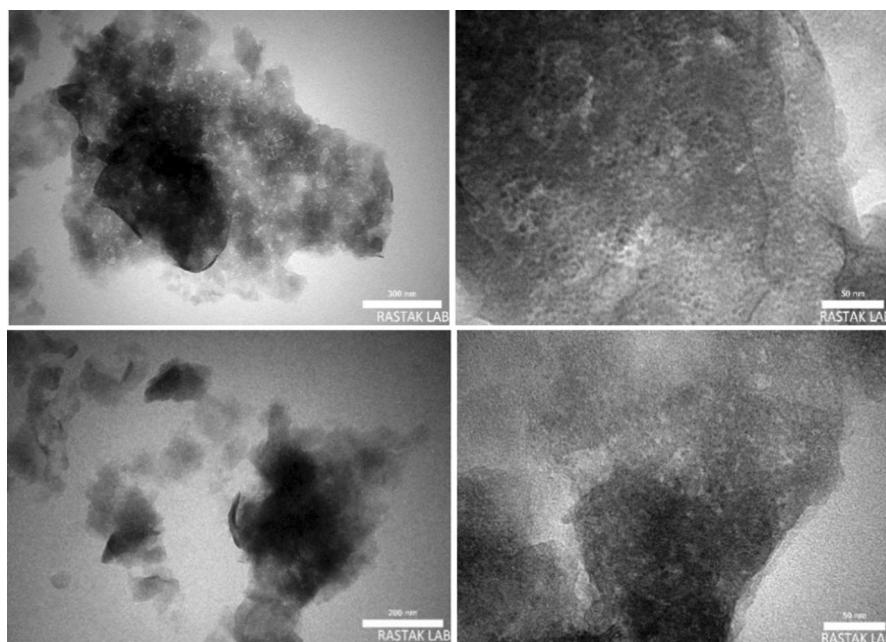
Fig. 4 TEM images of M-NiO nanocatalyst

Catalytic activity

The reaction of benzyl chloride, phenylacetylene and sodium azide in the presence of M-NiO nanocatalyst was chosen to optimize the reaction conditions. Various solvents like CH_3CN, EtOH, H_2O, and EtOH/H_2O (1: 1) were investigated. At room temperature, we did not get good results with various amounts of the catalysts and with each of the solvents after 3 h. It was found that the highest yield and lower reaction time acquired in water under reflux condition (Table 2). M-NiO nanocatalyst containing 7.87, 15.5 and 20 wt. % of NiO was prepared, and their performance on the model reaction studied. The catalyst contains about 7.87 wt. % NiO and exhibited the highest yield of reaction of about 93%. Moreover, the influence of catalyst amounts was explored. The reaction between benzyl chloride, phenylacetylene and sodium azide in the presence of 0.03 g of M-NiO nanocatalyst containing about 7.87 wt. % NiO, obtained the corresponding triazole in highest yield after 20 min under reflux condition (Table 2).

After optimization studies, it was found that molar ratios of 1, 1.1, 1.1, benzyl chloride, phenylacetylene and sodium azide were the best to achieve the highest yield of the desired product. Notably, in this process, there was no need for a base, reducing substance or any additive reagent when M-NiO nanocatalyst was employed. Furthermore, all the products were easily isolated by straightforward filtration and evaporation of the solvent. To study the scope of the procedure, the synthesis of various triazole derivatives was investigated (Table 3). Several alkyl or benzyl halides with both electron-withdrawing groups and electron-donating
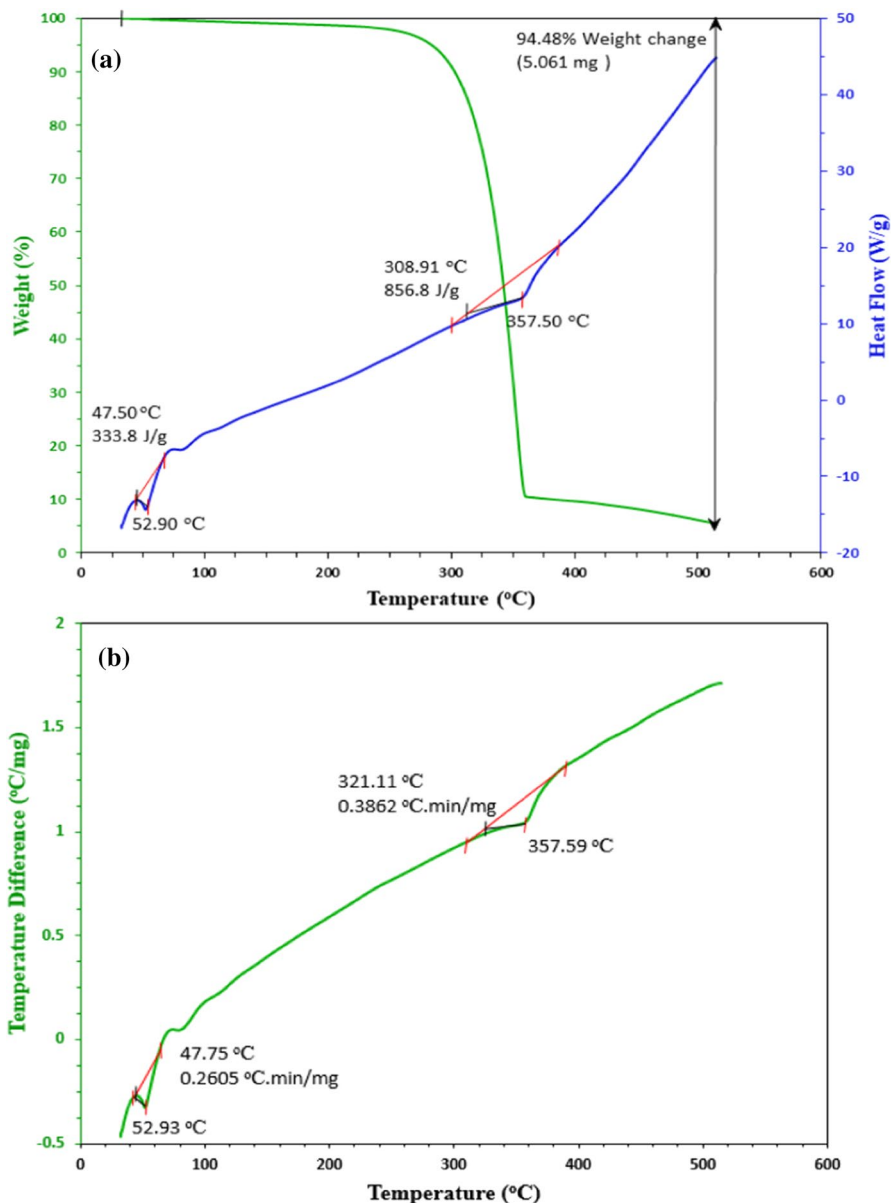
Fig. 5 TGA/DSC (**a**) and DTA (**b**) of M-NiO nanocatalyst

groups were subjected to the similar reaction conditions to synthesize the desired 1,2,3-triazole derivatives (Table 3). The results signified that benzyl bromides and benzyl chlorides were reacted under the optimized reaction conditions and corresponding products obtained in high yields. However, it was observed that benzyl bromides reacted faster than benzyl chlorides. Moreover, this procedure

Table 2 Optimization of the reaction conditions.[a]

Entry	Conditions	Catalyst amounts (g)	Time (min)	Yield (%)[b]
1	CH_3CN	0.03	120	Trace
2	CH_3CN	0.05	120	40
3	EtOH	–	120	–
4	EtOH	0.03	60	45
5	EtOH	0.05	60	60
6	H_2O	–	120	–
7	H_2O	0.01	120	55
8	H_2O	0.02	60	76
9	H_2O	0.03	20	93
10	H_2O	0.05	20	92
11	H_2O/EtOH	0.03	60	50
12	H_2O/EtOH	0.05	45	70

[a] The reaction was performed in the presence of M-NiO nanocatalyst containing 7.87 wt. % NiO under reflux conditions. [b] Isolated yield
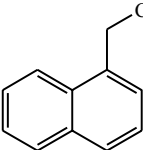
can be effectively applied for the synthesis of 1,4-disubstituted-1H-1,2,3-triazoles from some alkyl halides. All the corresponding triazoles were synthesized in high regioselectivities, and corresponding 1,4-disubstituted-1H-1,2,3-triazoles obtained in high yield. Regioselective synthesis of 1,4-disubstituted-1H-1,2,3-triazoles was confirmed by the appearance of a singlet in the region of 7.8–8.5 ppm for the trizole derived from benzyl halides in ^{1}H-NMR spectra which corresponds to the hydrogen on 5-position of triazole ring [36].

The reusability of the M-NiO nanocatalyst was also studied under the chosen model reaction. After reaction completion, the catalyst was separated and washed with hot ethanol. Then, the catalyst was dried and stored for another consecutive run. This process repeated for 6 runs. From Table 4, when the M-NiO nanocatalyst was recycled after six runs under optimized conditions, the isolated yield of the corresponding product was reduced only a few percent (6%).

In order to show the merit of the M-NiO nanocatalyst in comparison with other reported catalysts used for the synthesis of 1,2,3-triazoles, some of the obtained results are presented and compared in Table 5.

By comparing the results in the presence of M-NiO nanocatalyst with other catalysts, it was found that M-NiO nanocatalyst catalyzed the reactions efficiently in water without the need for any additional reagent such as base or reducing substance and the desired products were synthesized with high yields in short reaction times. In comparison with reported complex catalysts, M-NiO nanocatalyst is simple and its preparation is very easy. The reaction in the presence of other catalysts like Raney Ni has been performed in organic solvents such as toluene and required longer reaction times.

Table 3 Regioselective synthesis of 1,4-disubstituted-1H-1,2,3-triazoles catalyzed by M-NiO nanocatalyst in water.[a]

Entry	Substrate	Time (min)	Yield (%) [b]	M.P. (°C) [c]
1	$C_6H_5CH_2Cl$	20	93	131–131
2	4-Cl-$C_6H_4CH_2Cl$	20	93	150–152
3	2,4-Cl_2-$C_6H_3CH_2Cl$	22	90	147–149
4	4-Me-$C_6H_4CH_2Cl$	25	91	109–110
5	4-MeO-$C_6H_4CH_2Cl$	22	91	140–141
6	3-Me-$C_6H_4CH_2Cl$	20	92	109–111
7	4-NO_2-$C_6H_4CH_2Cl$	25	93	154–156
8	$C_6H_5CH_2Br$	15	92	128–130
9	4-Br-$C_6H_4CH_2Br$	20	91	152–154
10	2-Cl-$C_6H_4CH_2Br$	30	90	87–88
11	4-Me-$C_6H_4CH_2Br$	20	91	109–110
12	CH_3CH_2Cl	35	89	61–62
13	$CH_3CH_2CH_2CH_2Cl$	30	90	46–48
14	naphthyl-CH_2Cl	30	88	128–130

[a] Reaction conditions: substrate (1 mmol), phenyl acetylene (1.1 mmol), NaN_3 (1.1 mmol), M-NiO nanocatalyst (0.03 g), in water under reflux conditions. [b] Isolated pure products. [c] Products were characterized by comparison of their spectroscopic data and melting points with those reported in the literature [3, 8, 28]

Table 4 Recyclability study of M-NiO nanocatalyst

Run	1	2	3	4	5	6
Time (min)	20	20	20	25	30	45
Yield (%) [a]	93	92	92	90	88	87

[a] Isolated yield

Conclusion

In conclusion, we have reported the preparation and characterization of M-NiO nanocatalyst as a new, efficient and recyclable catalyst. The results of this research showed that M-NiO nanocatalyst could be a good alternative to conventional copper catalysts for the regioselective synthesis of 1,4-disubstituted-1H-1,2,3-triazoles in water. In this process, any additional substances like reducing reagent are not required. Moreover, the catalyst can be easily separated and recycled at least 6 times without significant decrease in its efficiency. Other advantages such as high yields of products, ease of work-up and the clean procedure should make this method an alternative and important addition for the regioselective synthesis of 1,4-disubstituted-1H-1,2,3-triazoles.

Table 5 Comparison between the catalytic activity of M/NiO nanocatalyst with some other catalysts on the synthesis of 1,2,3-triazoles

Entry	Catalyst	Conditions	Time (h)	Yield (%) [a]	Reference
1	(NHC) Copper (I)-catalyst	Water	2	27–32	7
2	[P_4-VP]$CuSO_4$/NaAsc	Water/t-BuOH	0.5–2	75–95	8
3	Cu(I)-complexed magnetic nanoparticle catalyst	EtOH/Water	2–5	81–93	11
4	Raney Ni	Toluene	10–12	89	20
5	Cp_2Ni	water/xantphos air/Cs_2CO_3	1.5	42–93	21
6	M/NiO nanocatalyst	Water	0.3–0.5	88–93	This work

[a] Isolated yield

References

1. D.R. Buckle, D.J. Outred, C.J.M. Rockell, H. Smith, H.B.A. Spicer, J. Med. Chem. **26**, 251 (1983)
2. R. Huisgen, Pure Appl. Chem. **61**, 613 (1986)
3. M. Rajabzadeh, R. Khalifeh, H. Eshghi, M. Sorouri, Catal. Lett. **149**, 1125 (2019)
4. T. Shamim, S. Paul, Catal. Lett. **453**, 136 (2010)
5. H. Naeimi, S. Dadashzadeh, M. Moradian, Res. Chem. Intermed. **41**, 2687 (2015)
6. A.A. Jafari, H. Mahmoudi, H. Firouzabadi, RSC Adv. **5**, 107474 (2015)
7. N. Touj, I. Özdemir, S. Yasar, N. Hamdi, Inorg. Chim. Acta. **467**, 21 (2017)
8. M.A. Karimi Zarchi, F. Nazem, J. Iran. Chem. Soc. **11**, 1731 (2014)
9. A. Keivanloo, M. Bakherad, M. Khosrojerdi, A.H, Amin, Res. Chem. Intermed. **44**, 2571 (2018)
10. M. Chetia, P. Singh Gehlot, A. Kumar, D. Sarma, Tetrahedron Lett. **59**, 397 (2018)
11. L. Mohammadi, M.A. Zolifgol, M. Yarie, M. Ebrahimini, K.P. Roberts, S.R. Hussaini, Res. Chem. Intermed. **45**, 4789 (2019)
12. S.F. Hamzavi, S. Gerivani, S. Saeedi, K. Naghdipari, G. Shahverdizadeh, Mol. Divers. **24**, 201 (2019)
13. C. Sharma, M. Kaur, A. Choudhary, S. Sharma, S. Paul, Catal Lett. **159**, 82 (2020)
14. I. Misztalewska-Turkowicz, K.H. Markiewicz, M. Michalak, A.Z. Wilczewska, J. Catal. **362**, 46 (2018)
15. J. McNulty, K. Keskar, R. Vemula, Chem. Eur. J. **17**, 14727 (2011)
16. D.V. Partyka, L. Gao, T.S. Teets, J.B. Updegraff III., N. Deligonul, T.G. Gray, Organometallics **28**, 6171 (2009)
17. Y. Zhou, T. Lecourt, L. Micouin, Angew. Chem. **122**, 2661 (2010)
18. L. Zhang, X. Chen, P. Xue, H.H.Y. Sun, I.D. Williams, K.B. Sharpless, V.V. Fokin, G. Jia, J. Am. Chem. Soc. **127**, 15998 (2005)
19. E. Rasolofonjatovo, S. Theeramunkong, A. Bouriaud, S. Kolodych, M. Chaumontet F. Taran, Org. Lett. **15**, 4698 (2013)
20. H.S.P. Rao, G. Chakibanda, RSC. Adv. **4**, 46040 (2014)
21. W.G. Kim, M.E. Kang, J.B. Lee, M.H. Jeon, S. Lee, J. Lee, B. Choi, P.M.S.D. Cal, S. Kang, J.M. Kee, G.J.L. Bernardes, J.U. Rohde, W. Choe, S.U. Hong, J. Am. Chem. Soc. **139**, 12121 (2017)
22. T.M. Dhameliya, H.A. Donga, P.V. Vaghela, B.G. Panchal, D.K. Sureja, K.B. Bodiwala, M.T. Chhabria, RSC Adv. **10**, 32740 (2020)

23. M. Shokouhimehr, S. Mahmoudi-Gom Yek, M. Nasrollahzadeh, A. Kim, R.S. Varma, Appl. Sci. **9**, 4183 (2019)
24. K. Zhang, K. Hong, J.M. Suh, T.H. Lee, O. Kwon, M. Shokouhimehr, H.W. Jang, Res. Chem. Intermed. **45**, 599 (2019)
25. M. Shokouhimehr, M. Shahedi Asl, B. Mazinani, Res. Chem. Intermed. **44**, 1617, (2018)
26. N. Motahharifar, M. Nasrollahzadeh, A. Taheri-Kafrani, R.S. Varma, M. Shokouhimehr, Carbohydr. Polym. **232**, 115819 (2020)
27. F.A. Westerhaus, R.V. Jagadeesh, G. WienhÖfer, M.M. Pohl, J. Radnik, A.E. Surkus, J. Rabeah, K. Junge, H. Junge, M. Nielsen, A. BrÜckner, M. Beller, Nat. Chemistry. **5**, 537 (2013)
28. M. Rajabi, J. Albadi, A.R. Momeni, Res. Chem. Intermed. **45**, 3879 (2020)
29. S.S. Saei Dehkordi, J. Albadi, A.A. Jafari, H.A. Samimi, Res. Chem. Intermed. **47**, 2527 (2021)
30. F. Ghadirian, A.R. Momeni, J. Albadi, Iran. J. Catal. **10**, 155 (2020)
31. J. Albadi, A. Alihoseinzadeh, M. Jalali, M. Shahrezaei, A. Mansournezhad, Mol. Catal. **440**, 133 (2017)
32. J. Albadi, M. Jalali, H.A. Samimi, Catal. Lett. **148**, 3750 (2018)
33. N. Kanagatha, N. Sivakumar, K. Gayathri, P. Krishnan, N.G. Renganathan, S. Gunasekaran, G. Anbalagan, Proc. Indian. Natn. Sci. Acad. **79**, 467 (2013)
34. E.W. Hughes, J. Am. Chem. Soc. **63**, 1737 (1941)
35. A. Rahdar, M. Aliahmadb, Y. Azizi, J. Nanostruct. **5**, 145 (2015)
36. M. Keshavarz, R. Badri, Mol. Divers. **15**, 957 (2011)

Publisher's Note Springer Nature remains neutral with regard to jurisdictional claims in published maps and institutional affiliations.